Effects of heat treatment and sintering additives on thermal conductivity and electrical resistivity in fine-grained SiC ceramics

Guo-Dong Zhan[a)]
Department of Chemical Engineering and Materials Science, University of California, Davis, California 95616

Mamoru Mitomo
National Institute for Materials Science, Namiki 1-1, Tsukuba-shi, Ibaraki 305, Japan

Amiya K. Mukherjee
Department of Chemical Engineering and Materials Science, University of California, Davis, California 95616

(Received 4 December 2001; accepted 12 June 2002)

The effects of heat treatment and sintering additives on the thermal conductivity and electrical resistivity of fine-grained SiC materials were investigated. The thermal conductivity and the electrical resistivity of dense SiC materials were measured at room temperature by a laser flash technique and a current-voltage method, respectively. The results indicated that the thermal conductivity and electrical resistivity of the SiC materials were dependent on the sintering additives and the resultant microstructure. Annealed materials with oxide additives developed microstructures consisting of elongated grains of various α/β–SiC polytypes. In contrast, annealed materials with oxynitride additives had microstructures consisting of fine equiaxed grains entirely of β–SiC phase. For the annealed materials with oxide additives the observed thermal conductivity was over 110 W/mK. For the annealed materials with oxynitride additives the observed value was 47 W/mK. The electrical resistivity of a hot-pressed material with oxide sintering additives decreased after annealing. For annealed materials with oxynitride additives, the electrical resistivity was even lower. High-resolution electron microscopy revealed a thin amorphous phase along the grain boundaries. Energy dispersive x-ray spectroscopy results showed that there was segregation of both Al and O atoms and a very small amount of Y atoms at grain boundaries. The results indicated that the chemistry and structure of the grain boundary has significant influence on thermal and electrical properties in SiC.

I. INTRODUCTION

Silicon carbide (SiC) is an important structural material due to its excellent chemical stability, wear resistance, and high-temperature mechanical properties.[1–4] It also is a potential electronic material.[5–8] The development of low-cost, high-quality, single-crystal SiC substrates has been pursued since the first Lely (nonseeded growth process) platelets were used to make devices.[7] Recently, the development of polycrystalline SiC for electronic device applications has been a subject of intense research.[9–16] As it has high thermal conductivity[10] and a thermal expansion coefficient (4×10^{-6}/°C) that is close to that of silicon (3×10^{-6}/°C), SiC is an almost ideal candidate for the substrate material in Si semiconductors. However, SiC is usually a semiconductor and lacks sufficiently high electrical resistivity for some applications. A thermal conductivity of 490 W/mK[5] has been reported for a high-purity single crystal. Also, a thermal conductivity of 270 W/mK and electrical resistivity of over 10^3 Ω cm at room temperature[9,10] have been reported for a polycrystalline SiC doped with BeO. However, environmental concerns regarding the use of toxic beryllium have prompted the investigation of alternative doping agents to achieve high thermal conductivity. For example, the thermal conductivity of a vapor-deposited SiC material was enhanced by boron doping and improved even further by subsequent annealing treatment.[13] Thermal conductivities of up to 235 and 90 W/mK were observed for a material with 0.15 wt%

a)Address all correspondence to this author.
e-mail: gzhan@uedavis.edu

Al_2O_3 and a material with Al_2O_3 and Y_2O_3 additives, respectively.[14,15] The electrical resistivity of these materials was not reported.

More recently, we have reported that liquid-phase-sintered SiC with rare-earth additives exhibits desirable thermal and electrical properties for an electronic substrate application.[17] In the present study, oxide and oxynitride additives were used to enhance densification of fine-grained SiC. A seeding technique and annealing treatment were used to control grain growth.[18–20] The thermal and electrical properties of these materials measured at room temperature are reported here. High-resolution electron microscopy (HREM) and energy dispersive x-ray spectroscopy (EDS) were used to examine the state and compositions at the grain boundaries and within the grains. The electrical and thermal properties were analyzed in terms of the geometry and chemistry of the microstructure and grain boundaries.

II. EXPERIMENTAL

The starting material was an ultrafine β–SiC powder with an average particle size of 90 nm (Sumitomo-Osaka Cement Co., Tokyo, Japan). Oxide and oxynitride additives were used. The oxide additive was a mixture of 7 wt% Al_2O_3 (99.9% pure, Sumitomo Chemical Co., Tokyo, Japan), 2 wt% Y_2O_3 (99.9% pure, Shin-Etsu Chemical Co., Tokyo, Japan), and 1.785 wt% $CaCO_3$ (high-purity grade, Wako Chemical Co., Osaka, Japan) that decomposes to 1 wt% CaO at high temperature. The oxynitride additive was a mixture of 42 wt% SiO_2 (reagent grade, Kanto Chemical Co., Tokyo, Japan), 10.9 wt% MgO (high-purity grade, Wako pure Chemical Industries, Ltd., Osaka, Japan), 23.7 wt% Y_2O_3 (99.9% pure, Shin-Etsu Chemical Co., Tokyo, Japan), 13.0 wt% Al_2O_3, and 10.4 wt% AlN (Grade F, Tokuyama Soda Co., Tokyo, Japan) powders. The oxynitride composition of $Y_{0.124}\ Mg_{0.160}\ Si_{0.414}\ Al_{0.302}\ O_{1.4}\ N_{0.151}$, designated as G1, was prepared by ball milling in hexane for 3 h using SiC media and a SiC container. A second mixture of 36.9 wt% Y_2O_3, 55.8 wt% Al_2O_3 and 7.3 wt% AlN powders was designated as G2. For the case of oxynitride additives, the incorporation of nitrogen atoms into the oxide glass modifies the physical properties by increasing softening temperatures, elastic modulus, and the hardness of the glasses.[21,22] Accordingly, Y–Mg–Si–Al–O–N (G1) and Y–Al–Si–O–N (G2) oxynitride glasses, which have appreciable SiC solubility, were selected as the grain-boundary phases. To directly compare the effects of the oxide or oxynitride additives on the thermal and electrical properties, the total additive amounts were kept the same (10 wt%).

For the oxide additives, either 2.7 wt% coarse α–SiC powder (A-1 grade, 0.45 μm, Showa Denko, Tokyo, Japan) or β–SiC powder (B-1, grade, 0.43 μm, Showa Denko, Tokyo, Japan) was added as a nuclei for grain growth, which corresponds to 3.0 wt% SiC powder. The ultrafine SiC powder was eventually blended with 10 wt% of these sintering additives. The powder mixture was dried and hot pressed at 1750 °C for 40 min under a pressure of 25 MPa in Ar atmosphere for the mixture with oxide additives and in N_2 atmosphere for the mixture with oxynitride additives. The hot-pressed materials were further annealed at different temperatures and for different times. The processing conditions and the resulting densities of the hot-pressed and annealed materials are given in Table I. The chemical vapor deposition silicon carbide (CVD-SiC) with β-phase polycrystalline and thermal expansion coefficient of 4.5×10^{-6}/°C was prepared in reactant gases of SiC_{14} and CH_4. The total impurities were less than 1 ppm, including Cu < 100 ppb, K < 60 ppb, Cr = 26 ppb, Mo < 40 ppb, and Fe = 35 ppb. The bending strength, Vickers hardness, and Young's modulus were 784 MPa, 34.3 GPa, and 490 GPa, respectively.

The density of the hot-pressed and annealed materials was determined by the Archimedes method using distilled water as an immersion medium. The materials were cut, polished, and then etched by a plasma of CF_4 containing 7.8% O_2. The microstructures were observed by scanning electron microscopy (SEM). Note that the observed surfaces for all materials were perpendicular to the hot-pressing direction. SEM micrographs were analyzed using image analysis (Model Luzex III, Nireco Co., Tokyo, Japan) to determine grain size and aspect ratio (R_{95}).[23] X-ray diffraction (XRD) patterns were

TABLE I. Sintering additives, processing conditions, and densities of fine-grained SiC ceramics.

Materials	Additives	Processing conditions	Density (g/cm^3)
SC0	Oxide additives + α–SiC seeds	HP: 1750 °C/40min	3.21
SC1	Oxide additives + α–SiC seeds	HP: 1750 °C/40min + HT: 1850 °C/4h	3.19
SC2	Oxide additives + β–SiC seeds	HP: 1750 °C/40min + HT: 1850 °C/4h	3.18
SC3	Oxynitride additives, G1	HP: 1750 °C/40min + HT: 2000 °C/3h	3.17
SC4	Oxynitride additives, G2	HP: 1750 °C/40min + HT: 2000 °C/3h	3.21
CVD-SiC	Reactant gases: SiC_{14} and CH_4	Chemical vapor deposition	3.21

HP: hot-pressing; HT: heat treatment.

made from finely ground samples. Volume fractions for each SiC polytype were calculated from the relative intensities of certain peaks.[24,25]

Disks used for diffusivity measurements were machined such that their diameters were 10 mm and their thickness approximately 2 mm. The disks were polished to uniform thickness across the sample. In each case, the disks were fabricated so the direction of heat flow would be parallel to the hot-pressing axis. Thermal diffusivity was measured at room temperature using the laser flash technique (Model TC-3000, ULVAC, Yokohama, Japan) after specimens were coated with a layer of carbon black to enhance the absorption of the laser beam on the front side. Thereby the sample front side was heated by a short laser pulse. The heat absorbed was transported by thermal diffusion processes described by Fourier's equation to the sample's rearside. There the temperature rise was recorded for the determination of thermal diffusivity. The specific heat was also measured with same apparatus by pulsed-laser flash. The relative value was determined by using a comparative method (JIS R1611, Japanese standard for measuring thermal conductivity). Thus, the thermal conductivity κ was determined according to the following equation:

$$\kappa = \rho C_p \alpha \quad , \tag{1}$$

where ρ is density, C_p is heat capacity, and α is thermal diffusivity of the solid.

The specimens used for the electrical resistivity measurements were the same specimens used for the measurements of thermal diffusivity. Electrodes were formed on the upper and lower sides of the disks by painting on a silver paste. To eliminate any surface current effect, a guard ring was also formed around the upper side electrode.

Microstructural analysis of the SC1 material was performed using transmission electron microscopy (TEM; Topcon 002BF, Tokyo, Japan) and EDS. A thin foil was prepared for TEM by the standard procedures of grinding, dimpling, and argon-ion-beam thinning. The nanostructure of grain boundaries was examined by HREM using a microscope with a point-point resolution of 0.18 nm at 200 kV. The elemental composition of grain boundaries was analyzed by EDS (Noran Voyager in the Topcon microscope with a probe size <0.5 nm). All EDS analysis were performed using the same effective counting time.

III. RESULTS

The SiC compositions doped with 7 wt% Al_2O_3, 2 wt% Y_2O_3, and 1 wt% CaO were hot pressed to densities >98% of theoretical density without difficulty at 1750 °C. The microstructure of the hot-pressed material [SC0, Fig. 1(a)] consisted of relatively fine equiaxed grains with an average diameter of 110 nm and an aspect ratio of 1.8. In the annealed material with α–SiC seeds doped with 7 wt% Al_2O_3, 2 wt% Y_2O_3, and 1 wt% CaO [SC1, Fig. 1(b)], the microstructure consisted entirely of elongated SiC grains with a diameter of 920 nm and an aspect ratio of 5.2. In contrast, the microstructure of the annealed SiC material with β–SiC seeds [SC2, Fig. 1(c)] consisted of 60 vol% of fine matrix grains with a diameter of 750 nm and an aspect ratio of 3.5 and 40 vol% of

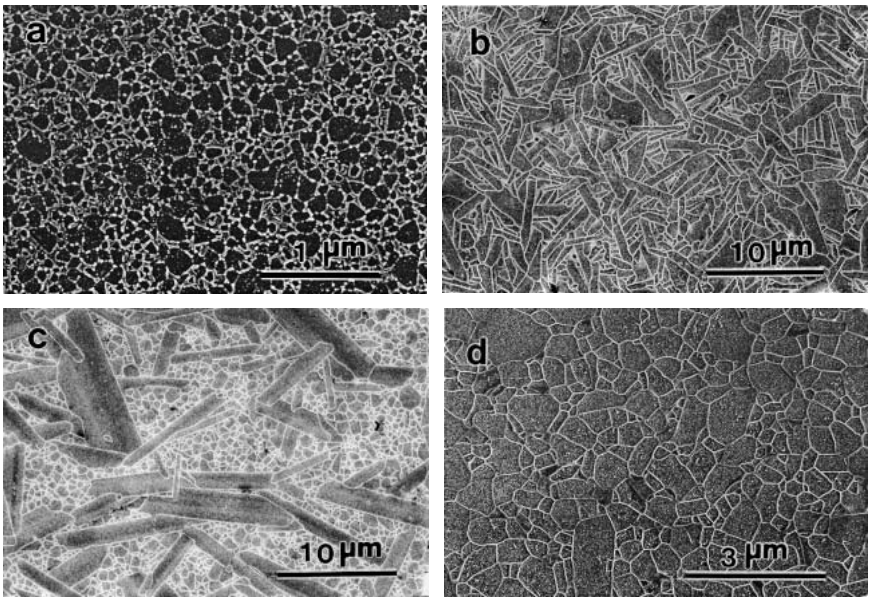

FIG. 1. SEM micrographs of polished and plasma etched specimens of (a) as-hot-pressed material, SC0; (b) annealed material with α-seeds, SC1; (c) annealed material with β-seeds, SC2; and (d) annealed material with G1, SC3.

large elongated grains with a diameter of 2.1 μm and an aspect ratio of 6.4. The SiC ceramics with the 10 wt% oxynitride additives of either G1 [SC3, Fig. 1(d)] or G2 (SC4) exhibited microstructures similar to each other consisting of fine SiC grains with $d \sim 500$ nm. Phase analysis showed that the annealed materials with α-seeds doped with oxide additives consisted of 57 vol% β–SiC and 43 vol% α–SiC, whereas the annealed materials with β–SiC doped oxide additives consisted of 75 vol% β–SiC and 25 vol% α–SiC. Moreover, the majority of the annealed material with α–SiC seeds was 6H, while 4H was the majority in the annealed material with β–SiC seeds. In contrast, no phase transformation occurred in the annealed materials with oxynitride additives (SC3 and SC4) due to the fact that oxynitride glass increases the stability region of β–SiC and suppresses β to α transformation in a nitrogen atmosphere.[26] Detailed data concerning the microstructural parameters and phase compositions are given in Table II.

The measured room-temperature thermal diffusivity and heat capacity and the calculated thermal conductivity of the SiC ceramics are shown in Table III. In comparison to the hot-pressed material, the thermal diffusivity greatly increased in the annealed materials with α and β seeds doped with oxide additives. The thermal diffusivity of the annealed materials with oxynitride additives is less than that of the materials with oxide additives. The heat capacity was slightly higher for the materials with oxide additives than those with oxynitride additives. The thermal conductivity of the materials with oxide additives (>110 W/mK) was far higher than that of the materials with oxynitride additives (47 W/mK). A maximum value of 115 W/mK for thermal conductivity was obtained for the material with β seeds doped with oxide additives. This value is similar to that reported for sintered SiC in Ref. 27. As shown in Table III, the CVD-SiC exhibited higher thermal conductivity (132 W/mK) than that of the present polycrystalline SiC systems. This value is higher than the report on CVD-SiC in Ref. 28 but lower than the report on CVD-SiC in Ref. 29.

As shown in Table III, these materials exhibited relatively higher electrical resistivity (>10^5 Ω cm). This is consistent with the report on hot-pressing SiC.[28] Moreover, electrical resistivity of the material doped with oxide additives was at least one order of magnitude higher than that of the material doped with oxynitride additives. However, the electrical resistivity of the hot-pressed material was far higher than that of the materials with oxide and oxynitride additives, even though thermal conductivity was the lowest. On the other hand, it is very interesting to note that the present CVD-SiC exhibited an extremely high electrical resistivity (up to 10^9 Ω cm) that is different from other CVD-SiC.[29,30]

Figure 2 is a TEM showing a representative microstructure for the annealed material with α seeds in which the elongation of the SiC grains is clearly visible. Amorphous grain boundary films were observed for the annealed material with α seeds by HREM, as shown in Fig. 3. All observed films appeared to be 1 nm thick. EDS was conducted to examine the chemical composition along and near the grain boundaries for the material SC1, with measurements taken from at least five interfaces. EDS spectra were obtained across the grain boundary at every 2 nm along the array of asterisks indicated

TABLE II. Polytypes and microstructural parameters of fine-grained SiC ceramics.

	Polytypes (vol%)			Microstructural parameters	
Materials	3C	6H	4H	d (μm)	R_{95}
SC0	93	0	7	0.11	1.8
SC1	57	40	3	0.92	5.2
SC2	75	5	20	2.10[a]	6.4
SC3	100	0	0	0.408	1.8
SC4	100	0	0	0.510	2.0

d is the average grain size; R_{95} is the aspect ratio.
[a]bimodal distribution, large grain only.

TABLE III. Measured thermal properties and electrical properties for SiC ceramics.

	Thermal properties			Electrical properties
Materials	Heat capacity C_p (J/gK)	Thermal diffusivity α (cm^2/s)	Thermal conductivity κ (W/mK)	Electrical resistivity ρ_v (Ω cm)
SC0	0.76	0.13	32	1.8×10^8
SC1	0.74	0.45	106	···
SC2	0.75	0.48	115	2.2×10^6
SC3	0.71	0.21	47	···
SC4	0.73	0.20	47	1.1×10^5
CVD-SiC	0.89	0.49	132	1.2×10^9

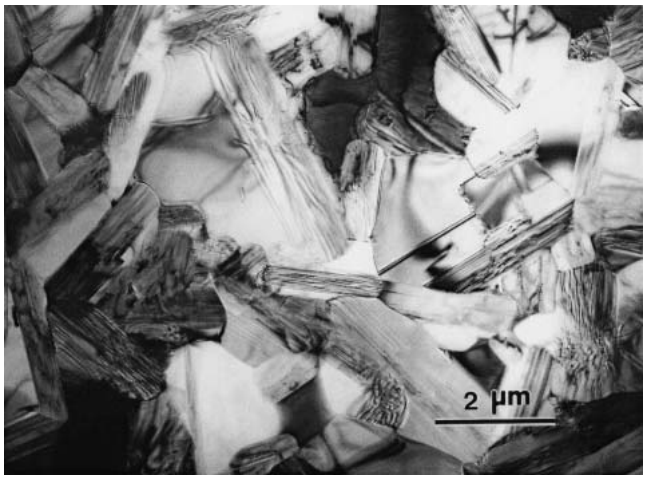

FIG. 2. A representative microstructure by TEM of the annealed material with α-seeds (SC1), showing elongation of the SiC grains.

in Fig. 3. The probe size for this analysis was 0.5 nm. Figure 4(a) is a profile for the atom fraction of Al within and near the grain boundary. It shows that Al atom was preferentially segregated along the amorphous grain boundary with a small amount into the SiC grains. However, very small amounts of Y atoms were observed at the grain boundary, as shown in Fig. 4(b). On the other hand, although O atoms were preferentially segregated along the grain boundary, a significant amount was found to be incorporated into the SiC grains. It should be pointed out that Ca was not detected along the grain boundaries or within the SiC grains for the present material. These differences in the compositions of the grains and grain boundaries have an important influence on thermal conductivity and electrical resistivity.

IV. DISCUSSION

The thermal conductivity of a material is a typical transport property; thus it is closely related to the microstructure of the material. The microstructure of SiC is dependent on sintering additives. The introduction of larger seed grains into the fine-grained SiC promoted grain growth. The annealed material with α seeds (SC1) exhibited a relatively uniform microstructure consisting mostly of elongated grains. In contrast, the annealed material with β seeds (SC2) had a duplex microstructure with fine matrix grains and much larger elongated grains.

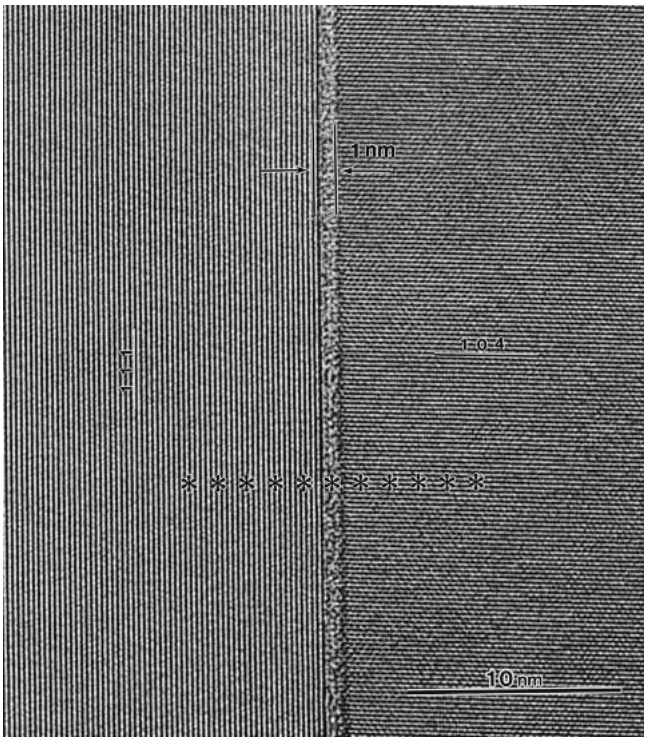

FIG. 3. High-resolution electron microscopy of the annealed material with α-seeds (SC1), showing an amorphous grain boundary film.

The SC1 and SC2 materials exhibited thermal conductivity values of 106 and 115 W/mK, respectively. On the other hand, the use of oxynitride additives completely suppressed β– to α–SiC phase transformation during annealing, as has been observed by others[31–33] and in our previous work.[34] A nitrogen atmosphere retards the phase transformation from β– → α–SiC and results in a fine microstructure, while an Ar atmosphere enhances the β → α phase transformation and the formation of a coarse microstructure. This is consistent with our present results. The microstructure of the materials with oxynitride additives consisted of fine, equiaxed grains with a continuous glassy interphase, leading to relatively low thermal conductivity value of 47 W/mK. Regardless of oxide or oxynitride additives, the heat capacity in these materials is almost the same, ranging from 0.71 to 0.76 J/gK,

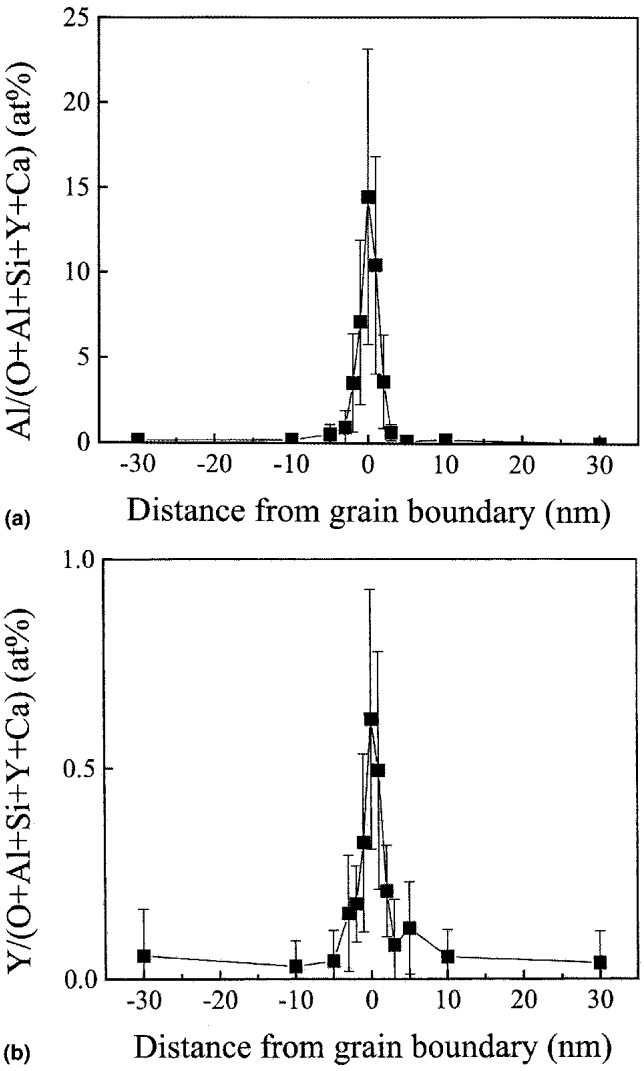

FIG. 4. EDS profiles at every 2 nm across the grain boundary for (a) the atom fraction of Al along and near the grain boundary and (b) the atom fraction of Y along and near the grain boundary for the annealed material with α-seeds (SC1).

consistent with sintered SiC materials.[27] These results suggest that the differences in the thermal conductivity of the materials with either oxide or oxynitride additives are due mainly to grain-boundary effect. Generally speaking, small grains lead to more extensive grain-boundary scattering.

SiC polytypes also exert an important influence on thermal conductivity.[12,15,16] The Al atoms in both 4H and 6H could substitute for Si because of the similar tetrahedral covalent radius of Al (0.126 nm) and Si (0.117 nm). The incorporation of Al into the SiC is in favor of β–SiC-to-4H phase transformation, as the solid solubility limit for 4H is higher than that for 6H. Thermal conductivity decreased with increasing contents of 4H polytype because the incorporation of the Al_2O_3 into the 3C–SiC grains leads to a solid–solution effect that reduces thermal conductivity. However, it is not reasonable, on this evidence alone, to interpret that the thermal conductivity in the present study for the material with β seeds, in which 4H was the major α–SiC, was higher than that of the material with α seeds in which 6H was the major of α–SiC. On the other hand, theoretically, a polycrystalline SiC material with a cubic structure is expected to exhibit the highest thermal conductivity due to the high symmetry and order in the crystal lattice. However, the materials with oxynitride additives consisted entirely of 3C polytype (cubic structure), but the thermal conductivity was quite low. Therefore, the dependence of thermal conductivity on the distribution of SiC polytypes was less pronounced for the present fine-grained materials.

In contrast to metals, in which electrons carry heat, SiC ceramics transport heat primarily by phonons. Point defects (i.e., substitute atoms, vacancies, and interstitial spaces) in the crystal greatly influence thermal conductivity. Such impurities are introduced either from the starting powder or from the sintering additives. The presence of impurities (dominated by Al and O) and vacancies significantly decreases thermal conductivity due to scattering of high-frequency phonons by point defects.[14] Therefore, the incorporation of some amount of Al and O into the SiC grains in the annealed material with α seeds (SC1) doped with oxide additives limited thermal conductivity. When materials were annealed in a nitrogen atmosphere and oxynitride additives were applied, the materials consisted entirely of β phase. The mechanism for the retarded phase transformation from β– → α–SiC is related to a reduced mass transport rate caused by lattice strains resulting from the introduction of nitrogen into the β–SiC.[31] Therefore, the lower thermal conductivity in the materials with oxynitride additives might be directly related to the incorporation of nitrogen into the SiC grains. The segregation along the grain boundary would also reduce thermal conductivity. These results indicate that thermal conductivity is influenced not only by the grain-boundary scattering but also by point-defect scattering due to the solid solution of Al, O, and N in the SiC grains in the present study.

Depending on impurities, SiC can be a *p*- or *n*-type semiconductor or an insulator with extrinsic ranges of $10 < \rho < 10^{12}$ Ω cm. The lower the carrier concentrations, the higher the electrical resistivity. The high electrical resistivity is likely due to the continuous grain-boundary insulating barriers.[9] The smaller the grain size, the more the grain boundaries, and the higher the electrical resistivity. This is consistent with the results for the materials with oxide additives but not for the materials with oxynitride additives. For example, the electrical resistivity in the material with oxynitride, which has a fine grain size, is lower than that in the material with oxide additives that has a coarse microstructure. Nitrogen either from the decomposition of additives or from the sintering atmosphere can dissolve into the SiC grains and act as the main electrically actived impurity[35] and thus lower both the thermal conductivity and electrical resistivity of SiC materials with oxynitride additives. These results suggest that electrical resistivity is related to both the grain boundary and the chemistry of the grain boundary. It is expected that increasing the thermal conductivity and electrical resistivity can be achieved by controlling the composition and heat treatment of the grain boundary and the solid-solution effect.

V. CONCLUSIONS

The annealed material with β seeds exhibited a higher thermal conductivity of 115 W/mK compared to the material with α seeds. On the other hand, the use of oxynitride additives completely suppressed β to α–SiC phase transformation during annealing. The microstructure in these materials consisted of fine, equiaxed grains, exhibiting low thermal conductivity (47 W/mK).

High electrical resistivity in the range of 10^5–10^8 Ω cm can be obtained in these annealed materials. The CVD-SiC material exhibits high thermal conductivity of 132 W/mK and extremely high electrical resistivity of 1.2×10^9 Ω cm.

The chemical compositions and microstructure (amorphous or crystallites) of the grain boundaries has the most influence on thermal and electrical properties of hot-pressed and annealed SiC.

ACKNOWLEDGMENT

One of the authors, Guodong Zhan, is presently supported by the United States Army Research Laboratory and the United States Army Research Office under Grant No. G-DAAD 19-00-1-0185.

REFERENCES

1. N.P. Padture and B.R. Lawn, J. Am. Ceram. Soc. **77,** 2518 (1994).
2. N.P. Padture, J. Am. Ceram. Soc. **77,** 519 (1994).
3. G-D. Zhan, M. Mitomo, and Y-W. Kim, J. Am. Ceram. Soc. **82,** 2924 (1999).
4. G-D. Zhan, R-J. Xie, M. Mitomo, and Y-W. Kim, J. Am. Ceram. Soc. **84,** (2001).
5. K. Moore and R.J. Trew, MRS Bull. **22**(3), 50 (1997).
6. R.C. Glass, D. Henshall, V.F. Tsvetkov, and C.H. Carter, Jr., MRS Bull. **22**(3), 30 (1997).
7. D.J. Larkin, MRS Bull. **22**(3), 36 (1997).
8. M.A. Capano and R.J. Trew, MRS Bull. **22**(3), 19 (1997).
9. Y. Takeda, K. Nakamura, K. Maeda, and Y. Matsushita, J. Am. Ceram. Soc. **70,** C-266 (1987).
10. Y. Takeda, Ceram. Bull. **67,** 1961 (1988).
11. S. Ogihara, K. Maeda, Y. Takeda, and K. Nakamura, J. Am. Ceram. Soc. **68,** C-16 (1985).
12. T. Sakai and T. Aikawa, J. Am. Ceram. Soc. **71,** C-7 (1988).
13. W. Kowbel, F. Gao, J.C. Withers, and G.E. Youngblood, J. Mater. Syn. And Proc. **4,** 195 (1996).
14. T. Kinoshita and S. Munekawa, Acta. Mater. **45,** 2001 (1997).
15. D-M. Liu and B.W. Lin, Ceram. Inter. **22,** 407 (1996).
16. M. Landon and F. Thevenot, J. Europ. Ceram. Soc. **8,** 271 (1991).
17. G-D. Zhan, M. Mitomo, R-J. Xie, and A.K. Mukherjee, J. Am. Ceram. Soc. **84,** 2448 (2001).
18. G-D. Zhan, M. Mitomo, H. Tanaka, and Y.W. Kim, J. Am. Ceram. Soc. **83,** 1369 (2000).
19. G-D. Zhan, Y. Ikuhara, M. Mitomo, R-J. Xie, T. Sakuma, and A.K. Mukherjee, J. Am. Ceram. Soc. **85,** 430 (2002).
20. Y-W. Kim, M. Mitomo, and G-D. Zhan, J. Mater. Res. **14,** 4291 (1999).
21. R.E. Loehman, J. Am. Ceram. Soc. **62,** 491 (1979).
22. S. Sakka, J. Non-Cryst. Solids **181,** 215 (1995).
23. M. Mitomo, H. Hirotsuru, H. Suematsu, and T. Nishimura, J. Am. Ceram. Soc. **78,** 211 (1995).
24. H. Tanaka and N. Iyi, J. Ceram. Soc. Jpn. **101,** 1313 (1993).
25. J. Ruska, L.J. Gauckler, J.L. Lorenz, and H.U. Rexer, J. Mater. Sci. **14,** 2013 (1979).
26. Y-W. Kim and M. Mitomo, J. Am. Ceram. Soc. **82,** 2731 (1999).
27. http://www.ceramics.nist.gov/srd/summary/scdscs.htm (2001).
28. http://www.ceradyne.com/dtsic.htm (2001).
29. http://www.cvdmaterials.com/sicprop1.htm (2001).
30. A.K. Collins, M.A. Pickering, and R.L. Taylor, J. App. Phys. **68,** (1990).
31. W.S. Seo, C.H. Pai, K. Koumoto, and H. Yanagida, Solid State Phenomena **25&26,** 133 (1992).
32. H-W. Jun, H-W. Lee, G-H. Kim, H-S. Song, and B-H. Kim, Ceram. Eng. Sci. Proc. **18,** 487 (1997).
33. M. Nader, F. Aldinger, and M.J. Hoffmann, J. Mater. Sci. **34,** 1197 (1999).
34. G-D. Zhan, M. Mitomo, Y-W. Kim, R-J. Xie, and A.K. Mukherjee, J. Mater. Res. **16,** 2189 (2001).
35. Y.A. Vodakov, G.A. Lomakina, E.N. Mokhov, V.G. Oding, and E.I. Padovanova, Sov. Phys. Solid State **20,** 258 (1978).